

The fraction of second generation stars in Globular Clusters from the analysis of the Horizontal Branch

F. D’Antona^{1*} and V. Caloi^{2 1*†}

¹ *INAF, Osservatorio Astronomico di Roma, Via Frascati 33, 00040 Monteporzio Catone (Roma), Italy.*

² *INAF, IASF–Roma, via Fosso del Cavaliere 100, I-00133 Roma, Italy*

Accepted . Received ; in original form

ABSTRACT

The majority of Globular Clusters show chemical inhomogeneities in the composition of their stars, apparently due to a second stellar generation in which the forming gas is enriched by hot-CNO cycled material processed in stars belonging to a first stellar generation. Clearly this evidence prompts questions on the modalities of formation of Globular Clusters. An important preliminary input to any model for the formation of multiple generations is to determine which is today the relative number fraction of “normal” and anomalous stars in each cluster. As it is very difficult to gather very large spectroscopic samples of Globular Cluster stars to achieve this result with good statistical significance, we propose to use the horizontal branch. We assume that, whichever the progenitors of the second generation, the anomalies also include enhanced helium abundance. In fact, helium variations have been recently recognized to be able to explain several puzzling peculiarities (gaps, RR Lyr periods and period distribution, ratio of blue to red stars, blue tails) in horizontal branches. We summarize previous results and extend the analysis in order to infer the percentage in number of the first and second generation in as many clusters as possible. We show that, with few exceptions, approximately 50% or more of the stars belong to the second generation. In other cases, in which at first sight one would think of a simple stellar population, we give arguments and suggest that the stars might all belong to the second generation. We provide in Appendix a detailed discussion and new fits of the optical and UV data of NGC 2808, the classic example of a multiple helium populations cluster, consistently including a reproduction of the main sequence splittings and an examination of the problem of “blue hook” stars. We also show a detailed fit of the totally blue HB of M 13, one among the clusters that are possibly fully made up by second generation stars. We conclude that the formation of the second generation is a crucial event in the life of globular clusters. The problem of the initial mass function required to achieve the observed high fraction of second generation stars can be solved only if the initial cluster was much more massive than the present one and most of the first generation low mass stars have been preferentially lost. As shown by D’Ercole et al. by modelling the formation and dynamical evolution of the second generation, the mass loss due to the explosions of the type II supernovae of the first generation may be the process responsible for triggering the expansion of the cluster, the stripping of its outer layers and the loss of most of the first generation low-mass stars.

Key words: globular clusters; chemical abundances; self-enrichment

1 INTRODUCTION

The observations of Globular Cluster (GC) stars are still to be interpreted in a fully consistent frame. Nevertheless, a general consensus is emerging on the fact that most GCs can not be considered any longer “simple stellar populations” (SSP), and that “self-enrichment” is a common feature among GCs. This consensus follows from the well known

* E-mail: dantona@oa-roma.inaf.it (FD); vittoria.caloi@iasf-roma.inaf.it (VC)

† This work has been supported through PRIN INAF 2005 “Experimenting stellar nucleosynthesis in clean environments” and PRIN MIUR 2007 “Multiple Stellar Populations in Globular Clusters: census, characterization, and origin”.

“chemical anomalies”, already noted in the seventies (such as the variations found in C and N abundances, the Na–O and Mg–Al anticorrelations). Recently observed to be present at the turnoff (TO) and among the subgiants (e.g. Gratton et al. 2001; Briley et al. 2002, 2004; Cohen et al. 2005), they must be attributed to some process of “self-enrichment” occurring at the first stages of the cluster life, as the same authors quoted above suggest. There was a first epoch of star formation that gave origin to the “normal” (first generation, hereinafter FG) stars, with CNO and other abundances similar to Population II field stars of the same metallicity. Afterwards, there must have been some other epoch of star formation (second generation, hereinafter SG), including material heavily processed through the CNO cycle. This material either comes entirely from the stars belonging to the first stellar generation, or it is a mixture of processed gas and pristine matter of the initial star forming cloud. We can derive this conclusion as a consequence of the fact that there is no appreciable difference in the abundance of elements such as Ca and the heavier ones between “normal” and chemically anomalous stars belonging to the same GC. Needless to say, this statement *does not* hold for ω Cen, which must indeed be considered a small galaxy and not a typical GC. In the following, we will only examine “normal clusters”, those which do not show signs of metal enrichment due to supernova ejecta. The homogeneity in the heavy elements is an important fact that tells us, e.g., that it is highly improbable that the chemical anomalies are due to mixing of stars born in two different clouds, as there is no reason why the two clouds should have a unique metallicity. In addition, the clusters showing chemical anomalies have a large variety in metallicities, making the suggestion of mixing of two different clouds even more improbable. The matter must have been processed through the hot CNO cycle, and not, or only marginally, through the helium burning phases, since the sum of CNO elements is the same in the “normal” and in the anomalous stars (e.g. Smith et al. 1996; Ivans et al. 1999; Cohen & Meléndez 2005). Carretta et al. (2005) find that actually the CNO is somewhat –but not much– larger in the SG stars of some GCs. Therefore, the progenitors may be either massive asymptotic giant branch (AGB) stars (e.g. Ventura et al. 2001, 2002)¹ or fast rotating massive stars (Decressin et al. 2007). In both cases, models show that the ejected material must be enriched in helium with respect to the pristine one. The higher helium content has been recognized to have a strong effect on horizontal branch (HB) morphology, possibly helping to explain some features (gaps, hot blue tails, second parameter) which, until now, have defied explanation (D’Antona et al. 2002). Along these lines, a variety of problems has been examined: the extreme peculiarity of the HB morphology in the massive cluster NGC 2808, (D’Antona & Caloi 2004); the second parameter effect in M 13 and M 3 (Caloi & D’Antona 2005); the peculiar features in the RR Lyr variables and HB of NGC 6441 and NGC 6388 (Caloi & D’Antona 2007).

The presence of strongly enhanced helium in peculiar HB stars has been confirmed, for NGC 2808 and NGC 6441, by spectroscopic observations (Moehler et al. 2004; Busso et al. 2007).

Beside this spectroscopic evidence, an unexpected feature has recently appeared from photometric data: the splitting of the main sequence in NGC 2808. After first indications from a wider than expected colour distribution (D’Antona et al. 2005), recent HST observations by Piotto et al. (2007) leave no doubt that there are at least three different populations in this cluster. This came after the first discovery of a peculiar blue main sequence in ω Cen (Bedin et al. 2004), interpreted again in terms of a very high helium content (Norris 2004; Piotto et al. 2005). The above mentioned cases can be considered as “extreme” ones, in the sense that no explanation had been attempted for them before the hypothesis of helium-enriched populations. Less critical situations, such as the HB bimodality in NGC 1851 and 6229, had been tentatively explained in terms of a unimodal mass distribution with a large mass dispersion ($0.055 - 0.10 M_{\odot}$, Catelan et al. 1998). But even such a rather artificial assumption could not help in the case of NGC 2808, which, as hinted before, finds a possible solution only in terms of varying helium in multiple stellar generations. Therefore, we consider appropriate to apply to the less peculiar cases the solution found plausible for the most peculiar ones. In fact, notice that split main sequences and strong bimodalities are only the tip of the iceberg of the self-enrichment phenomenon. In most clusters the higher helium abundances remain confined below $Y \sim 0.30$, and the presence of such stars would not be put in evidence either from main sequence observations (D’Antona et al. 2002; Salaris et al. 2006), or from a naïf interpretation of stellar counts on the HB, as we shall discuss in Sect. 4.1.

If we wish to shed light on the entire process of formation of GCs we must have a rough idea of the total number of SG stars. We will then analyze the HB in terms of populations differing in Y , using one or more of the following peculiar features:

- (i) bimodal HBs and HB gaps;
- (ii) presence of blue HB stars and very long period RR Lyr’s in high Z clusters;
- (iii) peaked number vs. period distribution of RR Lyr’s;
- (iv) blue–HB clusters.

In this paper we show the results of such an interpretation for several GCs. We start from a reanalysis of the NGC 2808 data, taking into account the results by Piotto et al. (2007) for the main sequence, and the ultraviolet HST data by Castellani et al. (2006); we summarize the results already published and discuss briefly the other clusters. The table of the derived FG and SG percentages is the basis to discuss the clusters’ dynamical evolution required to produce the high fraction of stars presently belonging to the SG.

2 THE BASIC MODEL

Here we summarize why and how a helium enrichment modifies the HB morphology (D’Antona et al. 2002), and the basic inputs of the HB and main sequence (MS) simulations adopted to constrain the FG and SG.

¹ If the Carretta et al. (2005) CNO data really indicate that a limited number of third dredge up (e.g. Iben & Renzini 1983) episodes plays a (small) role in the nuclear processing of the matter giving origin to the SG, the massive AGB progenitors are possibly favoured.

2.1 Red giant mass, mass loss, and helium content

The evolving mass in a GC is a function of age, metallicity and helium content. From the well defined turnoff of GCs, it is evident that any age spread must be much smaller than the global age (10-13 Gyr). In addition, the metallicity spread among cluster members are contained within $\sim 0.04\text{dex}$ ². Thus, once fixed age and metallicity, the evolving mass is a function of the helium content only, and it decreases when helium is increased. The dependence $\delta M_{RG}/\delta Y \sim -1.3 M_{\odot}$ is such that, e.g. the small increase in helium content from the primordial value $Y=0.24$ to the moderately higher $Y=0.28$ decreases the evolving mass by $\sim 0.05 M_{\odot}$.

During the latest phases of red giant evolution, both normal and helium enhanced stars lose mass. We assume that mass loss follows Reimers' law (Reimers 1975)

$$\dot{M}_R = 4 \cdot 10^{-13} \eta_R \frac{LR}{M} \quad (1)$$

where η_R is a free parameter directly connected with the mass loss rate and L, R and M are luminosity, mass and radius expressed in solar units. This expression has no explicit dependence on helium abundance or metallicity. While the independence from the metallicity may be questioned, the helium content, at the level of variation we are considering, should not affect the mass loss rate, as helium has no strong effect on surface opacities and possible grain formation. It turns out that also the total mass lost by giants with different helium content and similar age does not depend on the helium content. In fact, we computed tracks of stars with different helium content, and having different mass so that they have the same evolving age, and we find that *the total mass lost* differs only by $0.001 - 0.002 M_{\odot}$ when the models reach the helium flash. On the other hand, the helium core mass at the helium flash depends on the helium content, decreasing with increasing helium, but at a much smaller rate than the decrease of the red giant mass. Therefore, the ratio of core mass to the remnant mass is larger for larger Y, and these stars will occupy a position on the ZAHB at a bluer colour than stars with lower Y. This means that, if the cluster contains stars of FG with "standard" Y, and stars of SG with larger Y, these latter will be "bluer" than the FG stars.

Assuming the point of view that the HB contains stars with different helium content, the estimate of age and metallicity on the one side, and the HB morphology on the other, will indicate which part of the HB population belongs to the FG. This component should have a uniform helium content, probably close to the Big Bang abundance (e.g. $Y \sim 0.24$ Coc et al. 2004). For the FG of the most metal rich clusters we will assume a larger initial, uniform helium $Y=0.25$. On the contrary, the SG will most probably show a spread in Y, for two main reasons: the self-enriched material in fact 1)

may come from different progenitors, having different chemical peculiarities or 2) it may be diluted in different fractions with matter from the FG. In both cases the helium abundance may differ among the SG stars. Notice however that *if we have physical reasons (e.g. based on one of the peculiarities listed in Sect. 1) to attribute to a star a helium content larger than the helium of the FG, we know that this star belongs to a SG, even if its Y is not much larger*. Of course, the total amount of SG self-enriched gas differs if the derived Y does, or does not, result from dilution with pristine matter.

2.2 The grids of HB models

The basis of the synthetic HB distributions are stellar models computed with the code ATON2.0, described in Ventura et al. (1998) and Mazzitelli et al. (1999). The HB models have been evolved until the disappearance of helium in the convective core. We have adopted metallicity $Z=2 \cdot 10^{-4}$ for the metal poor GCs; $Z=10^{-3}$ and $Z=2 \cdot 10^{-3}$ for the intermediate metallicity clusters, which represent the majority of data sets, and $Z=6 \cdot 10^{-3}$ for the high metallicity clusters. The helium core mass of the models is set at the helium flash core mass of the previous evolution, determined by evolving models for each couple (Z, Y) for an age of $11 \cdot 10^9 \text{yr}$. The metallicities of individual clusters may be slightly different from those adopted here, but the main aim—to distinguish between normal-helium and enhanced-helium stars in the construction of the HB—can be satisfactorily achieved. We will see that the ratios FG/SG are well defined from gross characteristics of the HB, and not by minute details. We computed grids of models for $Y=0.24, 0.28, 0.32$ and 0.40 .

We computed HB models up to $T_{\text{eff}} \sim 31000\text{K}$, that is the usually accepted limit for standard ZAHB models resulting from a He-flash occurring at the red giant branch tip.

These models can not explain the extreme "blue hook" stars (T_{eff} up to $\sim 37000\text{K}$) present in ωCen , M54 (Rosenberg et al. 2004), NGC6388 (Busso et al. 2007) and NGC 2808 (Moehler et al. 2004), and generally explained as a result of the mixing of processed matter with the very small residual hydrogen envelope, consequent to a late ignition of the helium flash, along the white dwarf cooling sequence (Sweigart 1997; Brown et al. 2001). Mixing raises the helium (and carbon) abundance in the envelope (see also Cassisi et al. 2003) and the star settles at larger T_{eff} . In addition, D'Antona & Ventura (2007) have suggested that deep mixing occurs, independently from a late helium flash, along the RGB evolution of giants belonging to the very high helium population ($Y \sim 0.35 - 0.40$) as deep mixing in this case is not forbidden by the molecular weight discontinuity barrier. So, deep mixing may involve most of the very helium rich stars, and increase, even considerably, their surface helium abundance³.

² According to Gratton et al. (2004): "Low upper limits in the spread of the abundances of Fe (of the order of 0.04 dex, r.m.s.) have been found for several clusters from both spectroscopy and from the widths of main sequence (MS) and red giant branch (RGB) stars in the colour magnitude diagrams CMDs (for summary and discussion, see Suntzeff 1993). At present the verdict on Fe variations in CGs except ωCen must remain 'not proven'."

³ The hypothesis of deep mixing is useful to increase the probability of obtaining extreme HB and blue hook stars. If we use only the very late flash hypothesis, just a few stars could happen to have the appropriate envelope mass, such that they do not ignite the flash on the RGB, or do not leave a He-white dwarf remnant.

In order to simulate the possible late-flash induced mixing (and any other kind of deep mixing), for the set of $Z=0.001$ adopted to simulate the HB of NGC 2808, we computed tracks of very low masses for $Y=0.45, 0.50, 0.60, 0.70$ and 0.80 , having core mass $M=0.4676 M_{\odot}$, the helium core mass at the flash for the $Y=0.40$ models.

2.3 Main sequence and turnoff models

For comparison with the main sequence colour distribution in NGC 2808 by Piotto et al. (2007), we use the isochrones for $Z=10^{-3}$ and $Y=0.24, 0.28, 0.32$ and 0.40 described in D’Antona et al. (2005).

2.4 Simulations

We adopt an appropriate relation between the mass of the evolving giant M_{RG} and the age, as function of helium content and metallicity. The mass on the HB is then:

$$M_{HB} = M_{RG}(Y, Z) - \Delta M \quad (2)$$

ΔM is the mass lost during the RG phase. We assume that ΔM has a gaussian dispersion σ around an average value ΔM_0 and that both ΔM_0 and σ are parameters to be determined and do not depend on Y .⁴ Therefore the HB mass varies both due to the mass dispersion σ around the average assumed mass loss, and due to the dependence of the RG mass on the helium content. As the evolving mass *decreases* with increasing helium content, the stars with higher helium will populate bluer regions of the HB. In each cluster, we must identify the FG section of the HB (e.g., in NGC 2808 this is easily identified with the red clump). Then we assume a primordial ($Y=0.24$) or a minimum ($Y=0.25$) helium content for the fraction of HB stars considered to belong to the FG. This fraction can be adjusted in order to reproduce the features we attribute to the FG (e.g., the peaked RR Lyr period distribution in M3, see later). We then assume that the rest of HB stars has larger Y , and adopt different $N(Y)$ distributions in order to reproduce the other parts of the HB number vs. colour distributions, when available.

We fix ΔM_0 and σ , and extract random both the mass loss and the HB age in the interval from 10^6 yr to 10^8 yr, according to the chosen Y distribution. We thus locate the luminosity and T_{eff} along the evolution of the HB mass obtained. We identify the variable stars as belonging to a fixed T_{eff} interval and compute their period according to the pulsation equation (1) by Di Criscienzo et al.

⁴ A complication in the interpretation of HB morphologies, not included in this work, arises if not only the helium content between FG and SG varies, but *also the total CNO content*. This additional problem comes out from the observations of NGC 1851 (see Sect. 3.2) whose HR diagram shows a splitting in the sub-giant branch (Milone et al. 2008). While Cassisi et al. (2008) are able to explain this feature by assuming an SG with about double CNO content, and same age as the FG (thus in the classical self-enrichment scenario), the subsequent interpretation of the HB morphology by Salaris et al. (2008) can not be simply achieved by doubling the CNO, but it requires some extra mass loss for the SG stars. Here, our main aim is to find out the percentages of FG and SG, and this can be obtained also within the framework of our simpler assumptions.

(2004). The results are very similar if we adopt the classic van Albada & Baker (1973) relation. The real problem is given by the choice of the exact boundaries of the RR Lyr strip, that affect strongly the number and mean period of the RR Lyrae variables (see, e.g., the discussion in Caloi & D’Antona 2008).

The L and T_{eff} values are transformed into the different observational bands. As most observations are available in the B and V bands, and/or in the Bessell’s I, we derive the visual magnitude M_v and the B–V or V–I colours, using the transformations by Bessell, Castelli, & Plez (1998). Although our main aim—to understand the different fractions of FG and SG stars—is not affected by this problem, we remark that the B–V and V–I colours saturate at large T_{eff} . The bolometric corrections become very large, so the number vs. magnitude distribution may suffer some uncertainties, which can be avoided by using different magnitudes, e.g. the ultraviolet HST bands. We exemplify such comparisons for the case of the clusters NGC 2808 and M 13 in the Appendix A. The transformations for the ACS – HST bands are taken from Bedin et al. (2005). The WFPC2–HST relations are by Origlia & Leitherer (2000), plus additional transformations kindly provided by L. Origlia.

We associate a gaussian spread in colour and magnitude to each point, in order to simulate the impact of observational errors. We do not include binaries in the simulations. We mostly compare the theoretical simulations and the observations by looking at the number counts vs. colour in the horizontal part of the HB (e.g. for the red part and the RR Lyr) or vs. magnitude, for the vertical part, if the blue HB is very extended.

3 BIMODALITY AND GAPS IN THE HB

There is a huge literature which has defined and attempted to understand the gaps on the blue side of the HB (see, e.g. Ferraro et al. 1998; Piotto et al. 1999, and references therein). While a gap at $T_{\text{eff}} \sim 10^4$ K should probably be attributed to the operation of diffusion (Glaspey et al. 1989; Grundahl et al. 1999; Caloi 1999), other gaps may have to do with discontinuities in the helium content (D’Antona et al. 2005; Lee et al. 2005). In particular, a bimodal distribution in colour characterizes the HB of some clusters, that have well populated blue and red sides of the HB, with limited or null population of RR Lyr variables. NGC 2808 is a prototype of this class, and Catelan et al. (1998) were not able to interpret it in terms of a unique mass distribution, even with a mass spread as large as $0.3 M_{\odot}$. A multimodal mass distribution was then required to explain this HB.

The HB bimodality in NGC 2808 was the main hint used by D’Antona & Caloi (2004) to infer the presence of multiple stellar generations differing in Y in the cluster, an interpretation nicely supported by the subsequent observation of the main sequence splitting (D’Antona et al. 2005; Piotto et al. 2007). In addition, in this cluster are found the still mysterious “blue hook” stars. So NGC 2808 appears as an ideal benchmark for the application of the multiple population hypothesis. We summarize in the following our present understanding of its modeling, and extend it to other situations.

3.1 NGC 2808

If age, metallicity and mass loss are such that normal-helium, FG stars, populate a red clump, the SG stars with helium enhancement will tend to populate the bluer HB and the RR Lyr region. If there is a gap between the normal-helium stars and the *minimum* helium content of the second generation, the case of NGC 2808 may appear: a red clump (FG), almost no RR Lyr (due to the helium gap) and a blue HB with larger helium content (starting from $Y \sim 0.28$ according to D’Antona & Caloi 2004; D’Antona et al. 2005). In those papers, we had modelled the mass loss along the RG branch by assuming that the larger Y would provoke a slightly larger global mass loss, as the evolving giants with higher Y are less massive, and thus have smaller gravity (see, e.g. Lee, Demarque, & Zinn 1994). We have ascertained that this is not the case (Sect. 2.1), so the HB has to be modeled by assuming the same average mass loss for both normal Y and higher Y red giants. In addition, we try to model better the EBT2 and EBT3 (in the definition by Bedin et al. 2004) blue clumps, which contain the extreme HB (D’Cruz et al. 2000; Brown et al. 2001) and the “blue hook” stars (Moehler et al. 2004), respectively, and compare also simulations based on HST ultraviolet and visual bands. The details can be found in the Appendix. We show that the new simulations are consistent with both the triple MS by Piotto et al. (2007) and the HB star distribution. The main difference with respect to the analysis by D’Antona et al. (2005) is that the intermediate Y population is now clustered at $Y \sim 0.31$. The cluster again results divided into 50% normal-helium stars, and 50% helium enriched stars, although the very high helium ($Y \sim 0.385$) stars are only $\sim 15\%$.

3.2 NGC 1851, NGC 6229

Following the guidelines mentioned in Sect. 1, we take the point of view of interpreting clusters with a bimodal HB in terms of multiple populations, as in the “paradigmatic” case of NGC 2808. Catelan et al. (1998) and Borissova et al. (1999) describe the complex HB structure of the cluster NGC 1851 and NGC 6229, respectively: bimodal, with few RR Lyr variables, a gap on the blue HB and possibly some extreme blue HB members, at the luminosity of the turn-off. In NGC 6229, the number ratio of the red, variable and blue HB components are: B:V:R=0.59:0.08:0.33. The RR Lyr average period is of the OoI type. We assume therefore that the RR variables belong to the first generation, since they have the period appropriate to the metal and helium content expected for these stars. So we expect that roughly 41% of cluster members belong to the first generation and 59% to the second, helium-enriched one. The extra-helium allows these latter stars to reach the bluer positions beyond the variable region, to which they should have been confined by a chemical composition of $Y \sim 0.24$ and $Z \sim 0.001$. (See later the case of M3). Of course, not all the helium-enhanced stars will be found on the blue, and vice-versa, but the distribution will be substantially the one mentioned above.

Similarly, for NGC 1851 we have: B:V:R=0.30:0.10:0.60 (Catelan et al. 1998), or B:V:R \sim 0.32:0.12:0.56 (Walker 1998). In this case the RR Lyr are again Oosterhoff type

I, but their periods are longer, so that the variables may belong to the SG. Recently, this latter cluster has been discovered to harbour a double subgiant branch (Milone et al. 2008), that can be interpreted as the presence of an FG and SG with different total CNO abundances and same age (Cassisi et al. 2008). The “bright” subgiant branch contains $55 \pm 5\%$ of stars (Milone et al. 2008) and may correspond to the red part of the HB. Thus the FG should contain $\sim 55\%$ of the total cluster stars. As we already remarked, Salaris et al. (2008) analyze the HB stellar distribution, and are not able to fit the blue and red side of the HB with different helium (and CNO-Na abundances) and the same mass loss on the RGB. While modelling of this HB may require a database of HB tracks computed with different Y and different compositions in CNO, for our present purposes it is sufficient to see that the consistent bimodality of both the SGB and HB indicate the presence of an FG and SG, with the given proportions.

4 CLUSTERS WITH HIGH METALLICITY AND PECULIAR HB

4.1 NGC 6441 and NGC 6388

The case of the high metallicity cluster NGC 6441 has been fully discussed by Caloi & D’Antona (2007), who showed that very helium rich stars *are also present among the red clump stars*. The analysis is able to explain not only the anomalous long periods of the RR Lyr (Pritzl et al. 2003), but also the extension in magnitude of the red clump (any attempt to attribute this thickness to differential reddening has failed —Raimondo et al. (2002)), and the hot blue side of the HB. Therefore, the morphology requires helium enrichment not only for the bluer side of the HB, as we could naively think, but even for the red clump stars. The physical reasons for this interpretation is the following: helium core burning stars having high Y and Z make long loops from red to blue in the HB (Sweigart & Gross 1976). In fact, both the higher mean molecular weight —leading to a high H-burning shell temperature— and the high metallicity —leading to a stronger CNO shell— conspire towards the result that the H-shell energy source prevails with respect to the He-core burning. The consequent growth of the helium core leads the evolution towards the blue. Therefore, if we must explain the luminous (long period) RR Lyr by stars having high helium, the same stars will also populate the red clump: this is exactly what we observe: if the helium content is not as large as $Y \sim 0.35$ *in the red clump*, the HB finds no satisfactory explanation. The percentage of helium enriched stars is in this case $\sim 60\%$ for NGC 6441.

We performed a similar analysis for NGC 6388 (see Fig. 1). The main difference among the two clusters is that NGC 6388 seems to have a higher tail of very high helium ($Y > 0.35$) stars, reaching $\sim 20\%$.

There are other analyses for these clusters in the literature: Busso et al. (2007) consider as peculiar only the blue HB stars. This would limit the SG to $\sim 15\%$. Also Yoon et al. (2008) attribute the presence of a SG to the RR Lyr and hotter stars only. They seem to be able to obtain the RR Lyr long periods with only $Y \sim 0.3$, but we have no details about their models to understand this difference. Our

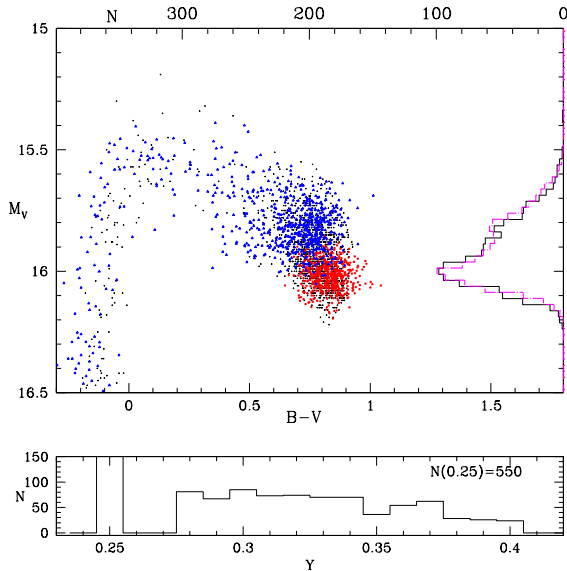


Figure 1. Synthetic HB simulation for NGC 6388. A similar analysis for NGC 6441 is shown in Caloi & D’Antona (2007). The HB data are taken from Piotto et al. (2002). In black we have the observations, while red and blue are the simulated stars. In red are the $Y=0.25$ stars, in blue those with $Y>0.25$ for a total of 1300 stars. The observed clump distribution (full line histogram) is shown on the right, superimposed to the theoretical distribution (dash-dotted histogram). The bottom panel shows the number vs. helium distributions assumed for the simulation. The number of stars with primordial helium $Y=0.25$, $N(0.25)$, is indicated in the label.

models require Y up to ~ 0.35 to fit the long periods of the RR Lyr, but, as explained above, this high Y also helps to reproduce a thickness $> 0.7\text{mag}$ of the red clump. On the other hand, Yoon et al. (2008) attribute the thickness of the red clump to differential reddening, a hypothesis in contrast with the data analysis by Raimondo et al. (2002).

4.2 47 Tuc

In 47 Tuc, the prototype of metallic GCs, the red clump is much less thick in magnitude than in the two anomalous clusters above. In Fig. 2 we show the histograms of the number of stars in the red clump of NGC 6441, NGC 6388 and 47 Tuc versus magnitude. The magnitudes have been normalized so that the peak in the distribution coincides for all the clusters. The “thickness” in magnitude of NGC 6388 and NGC 6441 is larger than for 47 Tuc. The excess of stars at smaller luminosities below the maximum is probably due to the larger observational errors, but the (asymmetric) excess at higher luminosities is most easily interpreted as due to stars with helium much higher than normal. Based on this feature only, we infer that the 47 Tuc SG should not be larger than $\sim 25\%$ of the stars. Observations show that CN strong and CN weak stars in the cluster are about in similar percentages (Briley et al. 2004), and if these two groups are to be interpreted as FG and SG, we have a contradiction. An escape from this problem can be found if the first stellar generation in 47 Tuc has a larger initial helium content (Salaris & Weiss 1998).

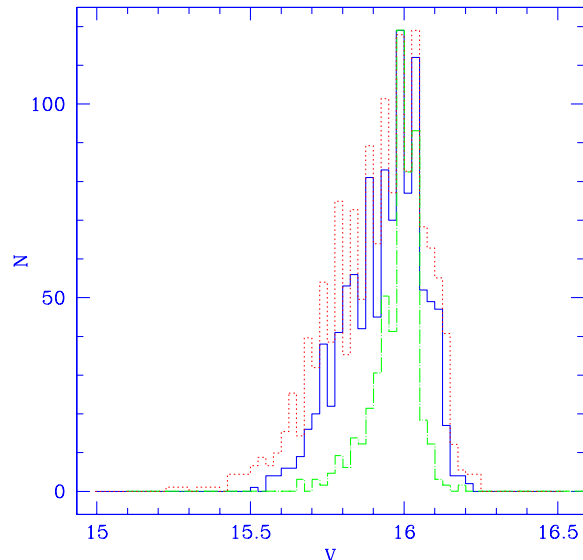


Figure 2. Plot of the observed number of stars versus magnitude for the red horizontal branch of three metal rich clusters: NGC 6441 (dots), NGC 6388 (full line), and 47 Tuc (dashed line). See text for the interpretation.

5 THE PEAKED PERIOD DISTRIBUTION OF RR LYR STARS

The prototype of HBs has often been considered the HB of the cluster M3: it is well populated both in the red part, in the RR Lyr’s and in the blue side, without a blue tail. The HB distribution among red, variable and blue members can be reproduced by assuming an average mass loss along the RGB, with a standard deviation $\sigma \sim 0.025 M_{\odot}$.

However, there are two important facts to be mentioned: i) the detailed colour distribution along the HB is by no means uniform, and ii) the RR Lyr period distribution appears strongly peaked, a feature that cannot be understood in terms of a more or less uniform mass distribution (Castellani & Tornambe 1981; Rood & Crocker 1989; Catelan 2004; Castellani et al. 2005). We have examined in detail this case (Caloi & D’Antona 2008); since there are several other clusters showing the same problem, we summarize the main points of the model for M3 and extend the interpretation to other clusters.

5.1 The period distribution of M 3

As said before, the RR Lyr period distribution in M 3 is highly peaked (see Figure 3, left side, full line histogram). Castellani et al. (2005) realized that the only way to reproduce this peak was to reduce the dispersion in the mass lost in the RGB. Once obtained the correct distribution with a given recipe for the mass loss, the authors had to assume a different average mass loss, with a different dispersion, to account for the blue side of the HB. In the hypothesis of multiple helium enhancements, the blue side is naturally populated by helium rich stars, as shown by Caloi & D’Antona (2008). In the simulations, we can explain both the period distribution and the colour distribution along the HB for the

Table 1. Helium history of clusters

Name	FG		SG		Extreme pop.		Data	Interpretation
	Y	%	Y	%	Y	%		
Bimodal HB (and gaps). Blue MS								
ω Cen	0.24	?		?	~ 0.38	$\sim 20 - 25$	1	2
NGC 2808	0.24	50	0.30-0.32	35	~ 0.38	15	3, 4	5, 6, this paper
NGC 1851	0.24	65	?	35			7, 8	9, this paper
NGC 6229	0.24	40	>0.30	60			7, 10	this paper
High Z – Anomalous HB								
NGC 6441	0.25	38	0.27-0.35	48	>0.35	14	11, 12, 14	13, 14
NGC 6388	0.25	39	0.27-0.35	41	>0.35	20	11, 14, 15	14, this paper
47 Tuc	0.25	75 (?)	0.27-.32	25 (?)			11	this paper
47 Tuc	0.27	50 (?)	0.29-.32	50 (?)			16	17, this paper
Peaked distribution of RR Lyr's periods								
M3	0.24	50	.26-.28	50			18, 19	20
M5	0.24	30	.26-.31	70			21	this paper
NGC 3201	0.24	63	.26 - 0.28	37			22	this paper
NGC 7006	0.24	72	0.25 - 0.275	28			23	this paper
M68	0.24	45	0.26 - 0.28	55			24	this paper
M15	0.24	20	0.26 - 0.30	80			25	this paper
Blue-HB clusters								
M53	0.24	0?	0.27-0.29?	100			26, 27	this paper
M13	0.24	0?	0.27-0.35	70	~ 0.38	30	28	29, this paper
NGC 6397	0.24	0?	0.28 (?)	100			30, 31, 32	this paper

(1) Bedin et al. (2004); Piotto et al. (2005); (2) Norris (2004); (3) Bedin et al. (2000); Castellani et al. (2006); (4) Piotto et al. (2007); (5) D'Antona & Caloi (2004); D'Antona et al. (2005); (6) Lee et al. (2005); (7) Catelan et al. (1998); Walker (1998); (8) Milone et al. (2008); (9) Cassisi et al. (2008); Salaris et al. (2008); (10) Borissova et al. (1999); (11) Piotto et al. (2002); (12) Pritzl et al. (2003); (13) Caloi & D'Antona (2007); (14) Busso et al. (2007); (15) Pritzl et al. (2002); (16) Briley et al. (2004); (17) Salaris & Weiss (1998); (18) Corwin & Carney (2001); (19) Ferraro et al. (1997); Buonanno et al. (1994); (20) Caloi & D'Antona (2008) (21) Sandquist & Bolte (2004) (22) Layden & Sarajedini (2003); Piersimoni et al. (2002) (23) Wehlau et al. (1999); (24) Walker (1994); (25) Clement et al. (2001); (26) Rey et al. (1998); (27) Martell et al. (2008); (28) Ferraro et al. (1998); (29) Caloi & D'Antona (2005); (30) Kaluzny (1997); (31) King et al. (1998); Richer et al. (2006); (32) Carretta et al. (2005); Bonifacio et al. (2002); Pasquini et al. (2008) Caloi & D'Antona (2008)

red, variable and blue regions. The analysis however poses another problem: we find that the dispersion in mass loss along the RGB must be at most $\sigma \sim 0.003 M_{\odot}$ to be consistent with the period distribution. The question remains whether this small dispersion is peculiar to M 3, or rather we have always been misled by the overall reproduction of the HB morphology, for which previous simulations (at constant Y) needed a dispersion in mass loss of some hundredths of M_{\odot} , as quoted before.

5.2 NGC 3201, NGC 7006, M5

We examined NGC 3201 according to the same scheme used for M 3, on the basis of the data by Layden & Sarajedini (2003) and Piersimoni et al. (2002). Unfortunately, the cluster is affected by differential reddening (von Braun & Mateo 2001, and references therein). While it is possible to per-

form reddening estimates for the single RR Lyrae variables (Sturch 1966, Blanco 1992; see Layden & Sarajedini 2003), the same is not so easy for non variable stars. In fact, when we tried to reconstruct the colour distribution on the HB, we found many non variable stars in the variable region. Therefore we did not attempt to reproduce the detailed colour distribution as we did for M 3, but only the RR Lyr period distribution and the overall division among red, variable and blue members.

We compared the period distributions in M 3 and in NGC 3201, using both the data by Piersimoni et al. and Layden & Sarajedini. Notwithstanding the large difference in the total numbers of variables with an established period (more than 200 variables in M 3, slightly more than 50 in NGC 3201), one finds a strong similarity in the period distributions (see Fig. 3, left side). So we have again a peaked distribution, and even a dip at the same period! Therefore the NGC 3201 solution is quite similar to the one for M 3.

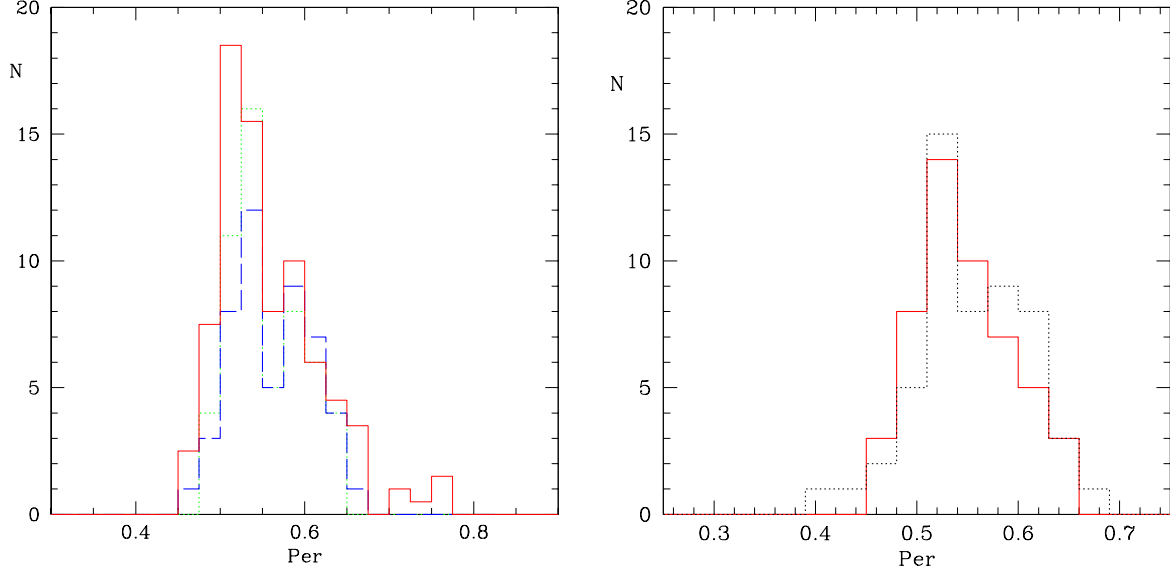


Figure 3. In the left figure we plot the number of RR Lyr vs. pulsation period for NGC 3201 from two different databases: dashed line, by Layden et al. 2003, and dotted by Piersimoni et al. 2002. We also plot the period distribution for M 3 (full line Corwin & Carney 2001), but these data have been divided by a factor two, in order to allow an easy comparison with NGC 3201. In spite of the different total numbers, the distributions are very similar. On the right we plot the NGC 3201 period distribution by Piersimoni et al. (dotted) and its simulation (full line), discussed in the text.

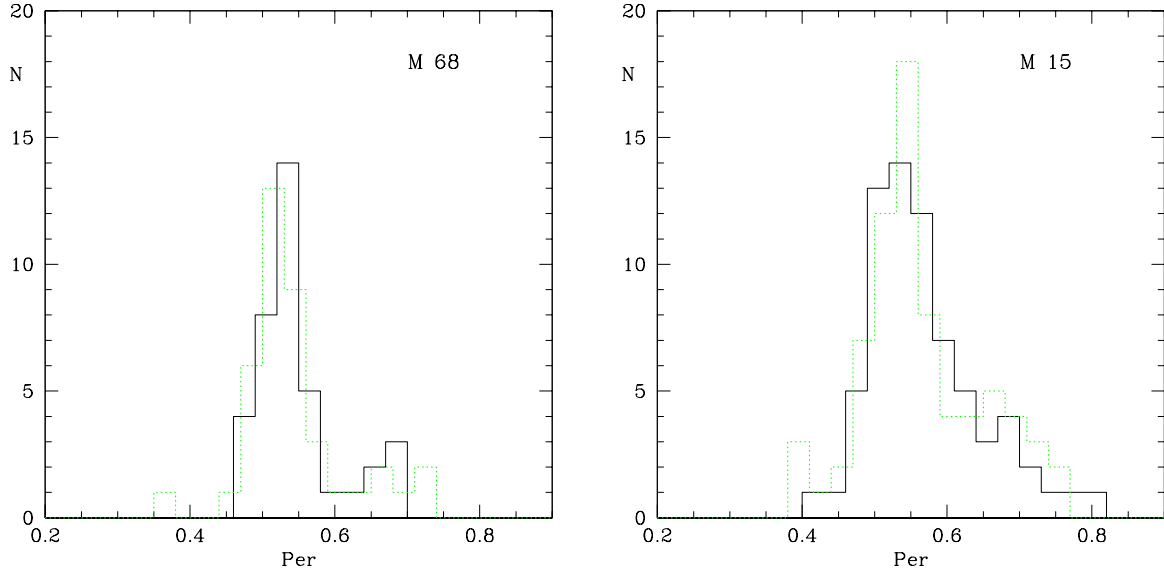


Figure 4. Period distribution fits for M 68 (left) and M 15 (right). Dotted histograms show the observed data, full line histograms are the simulations.

Our best simulations give 37% of HB members with helium enhanced from $Y=0.26$ to 0.28 , that is, coincident with the percentage of the blue HB stars. The mass dispersion optimum is even smaller than in M3 ($\sigma \sim 0.0015 M_{\odot}$). The period simulation is shown (full line histogram) in the right side of Fig. 3.

What said for NGC 3201 can be repeated for NGC 7006, whose RR Lyrs show again a peaked period distribution (Wehlau et al. 1999). Given the morphology of the HB, com-

posed mainly by red and variable stars, the required percent of helium enhanced objects is of about 27%, up to Y about 0.27.

The case of M 5 (NGC 5904) appears less simple, since the RR Lyrs period distribution presents two peaks. We can only approximate this distribution, while we succeed in reproducing the detailed colour distribution along the HB given by Sandquist & Bolte (2004). Within these limits, we estimate 70% of SG stars, up to a helium content of about

0.31 (we remind that M5 has more blue HB members than M 3, with the peak of population in the blue).

5.3 Very metal poor clusters: M 15 and M 68

A very good fit of the RR Lyr peaked period distribution in M 15 and M 68 is obtained with the same method adopted for M 3, but obviously using the tracks of metallicity $Z=2\times 10^{-4}$, adequate to describe these two clusters. The resulting period distributions are in Fig. 4. We must say that the fit of HR diagram, on the contrary, is much less successful than for the other clusters we have analyzed so far. The discrepancy is the following: the blue part of the HB in the simulations is achieved with Y in the range 0.26–0.28 for M 68, and 0.26–0.30 for M 15, but the luminosity of the blue side is too large with respect to the data. We suggest that helium is not the only parameter varying in these clusters, and that also the total CNO abundance should be varied, giving origin to a more complex description, still to be explored (see, e.g., the problem of NGC 1851 described above).

6 THE “BLUE-HB” CLUSTERS

A specially intriguing case is presented by the clusters with a prevalently blue HB, that is, with a HB type 1 – 2 (Dickens 1972). Almost – if not all – of them fall in the category of the classical “second parameter” problem. A fact that is not always considered as it deserves is that these clusters represent *the majority* of the population of the intermediate metallicity GCs (Alcaíno et al. 1999). So these clusters are not an exception, but rather the rule, that is, the most common result of the GC formation process. We shall examine some of these cases.

6.1 M 13: multiple populations, but all belonging the SG?

We analysed in detail the case of M 13, finding substantial support to the hypothesis that only the second star generation has survived in the cluster. This conclusion was reached on the basis of the relative positions of the turn-off, the red giant bump and the horizontal branch (Caloi & D’Antona 2005). This result, if confirmed, would be the first direct evidence for the presence of a substantial helium enhancement in GC stars. In the Appendix B we present a detailed analysis of the HB of this cluster, in the HST plane F555 vs. F336-F555 from Ferraro et al. (1998). The helium distribution is compared with the one necessary to reproduce the blue HB of NGC 2808, with the same assumption on age, metallicity and mass loss on the RGB. The comparison shows that M 13 stars have a shallower distribution in helium, but may have a peak at $Y\sim 0.28$, and a similar peak at $Y\sim 0.38$. In addition, *it completely lacks the red clump stars, that is the FG stars*. In the Ferraro et al. (1998) sample we use, there is a total of 221 HB stars, populating the upper, medium and low luminosity blue HB. According to the chosen simulation, a fraction 40% of stars has $Y=0.28-0.29$, another 30% has $Y\sim 0.31-0.35$, while the low HB is reproduced by taking $\sim 30\%$ of stars at $Y=0.38$. Thus the group of stars mostly

contributing to the RG bump is that at $Y=0.28-0.29$, as suggested in Caloi & D’Antona (2005). The conclusion is that in M 13 there are multiple populations, but, according to this interpretation of the data, they all belong to the SG!

On the other hand, several observations show the existence of chemically normal M 13 members, for example in Na abundance (e.g. Pilachowski et al. 1996) and in C and N abundances (e.g. Briley et al. 2004). However, if the $Y\sim 0.28$ population is the result of the dilution of pristine cluster matter ($Y=0.24$) with highly Y enriched matter ($Y\gtrsim 0.34$), as envisaged in many formation scenarios (Decressin et al. 2007; Ventura & D’Antona 2008b; D’Ercole et al. 2008), not necessarily the main chemical anomaly indicators will assume values noticeably different from those of the FG stars.

The analysis of the relative positions of the turn-off, the red giant bump and the HB could not be performed on other blue-HB clusters, due to the lack of a consistent photometry for these features. Clearly a possibility is that in all the clusters of this group most of the first generation stars have been lost. There are contradictory spectroscopic indications in favour or against this hypothesis. In the cluster NGC 6752, out of nine dwarfs and nine subgiants analyzed by Carretta et al. (2005), only one (subgiant) has a normal nitrogen content, all the others are substantially N-enriched ($[N/Fe]\sim 1-1.7$). The recent new data by Yong & Grundahl (2008), on the contrary, contain also nitrogen normal stars. This cluster could be similar to M13, also in having a very helium rich population producing the extreme HB stars.

6.2 NGC 6397, M53: apparently SSPs, but possibly SG-SSP?

Notice that NGC 6397 has $[Fe/H]=-2$ (Gratton et al. 2001) and so is not an intermediate metallicity cluster. It has a short blue HB, lacking extreme HB and blue hook stars, and its HR diagram has always been regarded as a perfect example of SSP, especially following the exceedingly refined HST proper motion selected observations by King et al. (1998) and Richer et al. (2006). Nevertheless, only three subgiants out of 14 stars are nitrogen normal (Carretta et al. 2005), leading us to suspect that the material from which these stars formed is CNO processed and thus of SG. This occurrence had already been noticed in Bonifacio et al. (2002), with reference to the paradox that nitrogen rich stars had almost-normal lithium content (see also Pasquini et al. 2008).

The above considerations lead naturally to the question: the simple population GC – one chemical composition, one age, of which one used to speculate until very recently – does it exist? We are inclined to give a negative answer. Let us consider the observations by Li & Burstein (2003), who took integrated spectra of eight galactic GCs, ranging in metallicity from $[Fe/H]\lesssim -2$ to $[Fe/H]\sim -0.8$, and showing a variety of HB morphologies (the clusters are: M 15, M 92, M 53, M 2, M 3, M 13, M 5, M 71). All these cluster show a substantial N-enhancement with respect to field stars of the same metallicity. Since we are dealing with integrated spectra, the result can not be directly interpreted in terms of percentage of second generation stars, that would be composed by nitrogen rich (CN or CNO cycled) matter. Nevertheless, the N-excess with respect to the field is a clear

indication that *at least* a certain amount of stellar matter is not the original one, in all the eight GCs quoted above.

The case of M 53 presents some interesting features. It is a very metal poor ($[\text{Fe}/\text{H}] \sim -2$, Zinn 1985, Harris 2003), massive cluster ($M_v = -8.70$ mag). Out of a total of 307 observed HB members (Rey et al. 1998), 257 are located blueward of, 35 within, and 12 redward of the RR Lyr instability strip, the bluest stars being located at $(B-V) \sim -0.08$. Three stars appear separated at bluer colours. So, the HB has a very short extension in colour, with most of its members concentrated at $(B-V) \sim 0.05$. This star distribution is unique among very metal poor GCs – see, f.e., Table 13 in Walker (1994). In fact: in M 15, a massive and high central density cluster, the 155 HB members are distributed from redward of the RR Lyrs to very blue colours and low visual luminosity, reaching the TO magnitude; M 68, a relatively small and not very concentrated cluster, exhibits a short HB from the red region to about $(B-V) \sim -0.1$ mag, with almost equal numbers of blue on the one side, and red and variable stars, on the other.

The extraordinary star concentration in a small colour interval suggests that the largest part of the HB population in M 53 can be obtained assuming a dispersion in the mass loss of $\sim 0.01 M_\odot$; a more precise photometry could give more stringent limits to the dispersion. On this basis, M 53 would appear a good candidate for a “normal”, first-generation-only cluster, but for the N-enhancement and the (mild) intrinsic spread in CN bandstrength (Martell et al. 2008). These chemical properties suggest that we are likely dealing with a one-generation cluster, but one in which the star generation we observe is the *second* one, and not the first.

Of course a final answer to the initial question will have to wait the investigation of the whole body of Galactic GCs, but since now secondary episodes of star formation appear widespread and crucial for building-up the clusters themselves.

7 CONCLUSIONS: HOW DID THE GCS FORM?

In all GCs examined in this work, a large fraction of the stellar population takes origin from secondary star formation episodes. Notice that we have examined only a fraction of the clusters with HB morphology or RR Lyr period distributions similar to those described here, so that we can suggest that the results of this work probably hold for a larger population of Galactic GCs. While the most massive clusters have extreme helium enhancements, also moderately massive clusters show a considerable degree of helium variation.

We reached our goals by examining in detail GCs that have unexplained features in their HBs, and extending the results to clusters with similar features. The HB morphology is one of the important features: clusters having a bimodal or multimodal HB are most easily interpreted by the coexistence of multiple generations with different helium content. Also a unique SG, whose stars had different degrees of mixing with pristine matter and thus ended up with different helium contents, is a possible solution. In any case, the extreme helium rich populations (in ω Cen and NGC 2808 at

least) are neatly separated from the other MS stars so that they should have a well defined independent origin.

Further, we used the period distribution of RR Lyrs in several clusters in order to reject the hypothesis of a unique Y value with a relatively large spread of mass loss on the RGB, that has been the standard way of interpreting the whole HB colour extension, but is inconsistent with most period distributions.

We re-examined in detail the HB distribution in NGC 2808, and obtained a helium distribution consistent with the main sequence recent data by Piotto et al. (2007). Also the UV data of this cluster find a good interpretation in terms of population with varying helium content, if we make the further hypothesis of deep mixing to understand the location of the blue hook stars. We also show that simulation of M 13 UV data is well explained with populations having different helium.

After this analysis, then, we must face the problem that the SG formation is not a peculiarity of a few very massive clusters, but must be the normal way in which a GC is formed in our Galaxy. It is almost obvious, and has often been discussed in the literature, that the ejecta of a unique first stellar generation with a normal initial mass function (IMF) can not produce enough mass to give origin to such a large fraction of second generation stars (see, e.g., the case made by Bekki and Norris (2004), for the blue main sequence of ω Cen). The only solution to the IMF problem is that *the starting initial mass from which the first generation remnant mass* (at least a factor 10 to 20 larger), so that the processed ejecta of the first generation provide enough mass to build up the second one. There are two possible ways of producing this result: the first possibility is that all these GCs formed within a dwarf galaxy environment (Bekki & Norris 2006; Bekki et al. 2007). There, GCs may be formed by mixing of pristine gas with the winds of the very numerous massive AGB stars evolving in the field of the dwarf galaxy, and later on the dwarf galaxy is dynamically destroyed. A second possibility has been recently suggested by D’Ercole et al. (2008). They show that the SG stars are preferentially born in the inner core of a FG cluster, where a cooling flow collects the gas lost by the FG stars. The massive stars that explode as SN II were preferentially concentrated in the cluster core. After the mass loss due to the supernovae type II explosions, the cluster expands, and begins losing the stars —mainly of FG— going out of the tidal radius. Thus the cluster may be destroyed, unless the gas lost by the most massive AGB stars begins collecting in the core and forms the SG, that initially does not take part in the cluster expansion. The study of the cluster dynamical evolution, followed by means of N-body simulations, shows that the cluster preferentially loses FG stars; these simulations show that high SG/FG number ratio can be achieved and SG-dominated clusters may survive.

8 ACKNOWLEDGMENTS

Many colleagues contributed to this analysis in several ways: we thank G. Bono for the HST UV data for NGC 2808, and F. Ferraro for the M 13 HST data. S. Cassisi helped by providing the colour transformations. Conversations and a long

collaboration with A. D’Ercole and E. Vesperini convinced one of us (FD) that the SG is a necessary ingredient for the survival of globular clusters.

REFERENCES

- Alcaíno, G., Liller, W., Alvarado, F., Mironov, A., Ipatov, A., Piskunov, A., Samus, N., & Smirnov, O. 1999, *A&AS*, 136, 461
- Bedin, L. R., Piotto, G., Zoccali, M., Stetson, P. B., Saviane, I., Cassisi, S., & Bono, G. 2000, *A&A*, 363, 159
- Bedin, L. R., Piotto, G., Anderson, J., Cassisi, S., King, I. R., Momany, Y., & Carraro, G. 2004, *ApJ Letters*, 605, L125
- Bedin, L. R., Cassisi, S., Castelli, F., Piotto, G., Anderson, J., Salaris, M., Momany, Y., & Pietrinferni, A. 2005, *MNRAS*, 357, 1038
- Bekki, K., & Norris, J. E. 2006, *ApJ*, 637, L109
- Bekki, K., Campbell, S. W., Lattanzio, J. C., & Norris, J. E. 2007, *MNRAS*, 377, 335
- Bessell, M. S., Castelli, F., & Plez, B. 1998, *A&A*, 333, 231
- Blanco, V. M. 1992, *AJ*, 104, 734
- Bonifacio, P., et al. 2002, *A&A*, 390, 91
- Borissova, J., Catelan, M., Ferraro, F. R., Spassova, N., Buonanno, R., Iannicola, G., Richtler, T., & Sweigart, A. V. 1999, *A&A*, 343, 813
- Briley, M., Cohen, J. G., & Stetson, P. B. 2002, *ApJ*, 579, L17
- Briley, M. M., Harbeck, D., Smith, G. H., & Grebel, E. K. 2004, *AJ*, 127, 1588
- Brown, T. M., Sweigart, A. V., Lanz, T., Landsman, W. B., & Hubeny, I. 2001, *ApJ*, 562, 368
- Buonanno, R., Corsi, C. E., Buzzoni, A., Cacciari, C., Ferraro, F. R., & Fusi Pecci, F. 1994, *A&A*, 290, 69
- Busso, G., et al. 2007, *A&A*, 474, 105
- Caloi, V. 1999, *A&A*, 343, 904
- Caloi, V. & D’Antona, F. 2005, *A&A*, 421, 95
- Caloi, V. & D’Antona, F. 2007, *A&A*, 463, 949
- Caloi, V. & D’Antona, F. 2008, *ApJ*, 673, 847
- Carretta, E., Gratton, R. G., Lucatello, S., Bragaglia, A., & Bonifacio, P. 2005, *A&A*, 433, 597
- Cassisi, S., Schlattl, H., Salaris, M., & Weiss, A. 2003, *ApJ*, 582, L43
- Cassisi, S., Salaris, M., Pietrinferni, A., Piotto, G., Milone, A. P., Bedin, L. R., & Anderson, J. 2008, *ApJ*, 672, L115
- Castellani, V., & Tornambe, A. 1981, *A&A*, 96, 207
- Castellani, M., Castellani, V., & Cassisi, S. 2005, *A&A*, 437, 1017
- Castellani, V., Iannicola, G., Bono, G., Zoccali, M., Cassisi, S. & Buonanno, R. 2005, *A&A*, 446, 569
- Catelan, M., Borissova, J., Sweigart, A. V., & Spassova, N. 1998, *ApJ*, 494, 265
- Catelan, M. 2004, *ApJ*, 600, 409
- Clement, C. M., et al. 2001, *AJ*, 122, 2587
- Coc, A., Vangioni-Flam, E., Descouvemont, P., Adahchour, A., & Angulo, C. 2004, *ApJ*, 600, 544
- Cohen, J. G., & Meléndez, J. 2005, *AJ*, 129, 303
- Cohen, J. G., Briley, M. M., & Stetson, P. B. 2005, *AJ*, 130, 1177
- Corwin, T. M., & Carney, B. W. 2001, *AJ*, 122, 3183
- D’Antona, F., Caloi, V., Montalbán, J., Ventura, P., & Gratton, R. 2002, *A&A*, 395, 69
- D’Antona, F. & Caloi, V. 2004, *ApJ*, 611, 871
- D’Antona, F., Bellazzini, M., Caloi, V., Fusi Pecci, F., Galletti, S., & Rood, R. T. 2005, *ApJ*, 631, 868
- D’Antona, F., & Ventura, P. 2007, *MNRAS*, 379, 1431
- D’Cruz N.L., O’Connell R.W., Rood R.T., Whitney, J.H. et al. 2000, *Apj*, 530, 352
- Decressin, T., Meynet, G., Charbonnel, C., Prantzos, N., & Ekström, S. 2007a, *A&A*, 464, 1029
- D’Ercole, A., Vesperini, E., D’Antona, F., Mc Millan, S. & Recchi, S. 2008, submitted to *MNRAS*
- Dickens, R. J. 1972, *MNRAS*, 157, 281
- Di Criscienzo, M., Marconi, M., & Caputo, F. 2004, *ApJ*, 612, 1092
- Ferraro, F. R., Carretta, E., Corsi, C. E., Fusi Pecci, F., Cacciari, C., Buonanno, R., Paltrinieri, B., & Hamilton, D. 1997, *A&A*, 320, 757
- Ferraro, F. R., Paltrinieri, B., Pecci, F. F., Rood, R. T., & Dorman, B. 1998, *ApJ*, 500, 311
- Glaspey, J. W., Michaud, G., Moffat, A. F. J., & Demers, S. 1989, *ApJ*, 339, 926
- Gratton, R. G., Bonifacio, P., Bragaglia, A., et al. 2001, *A&A*, 369, 87
- Gratton, R., Sneden, C., & Carretta, E. 2004, *ARA&A*, 42, 385
- Grundahl, F., Vandenberg, D. A., & Andersen, M. I. 1998, *ApJ*, 500, L179
- Grundahl, F., Catelan, M., Landsman, W. B., Stetson, P. B., & Andersen, M. I. 1999, *ApJ*, 524, 242
- Iben, I., Jr., & Renzini, A. 1983, *ARA&A*, 21, 271
- Ivans, I.L., Sneden, C., Kraft, R.P., et al., 1999, *AJ*, 118, 1273
- Kaluzny, J. 1997, *A&AS*, 122, 1
- King, I. R., Anderson, J., Cool, A. M., & Piotto, G. 1998, *ApJ*, 492, L37
- Layden, A. C., & Sarajedini, A. 2003, *AJ*, 125, 208
- Lee, Y., Demarque, P., & Zinn, R. 1994, *ApJ*, 423, 248
- Lee, Y.-W., et al. 2005, *ApJ Letters*, 621, L57
- Li, Y., & Burstein, D. 2003, *ApJ*, 598, L103
- Maeder, A., & Meynet, G. 2006, *A&A*, 448, L37
- Marcolini, A., Sollima, A., D’Ercole, A., Gibson, B. K., & Ferraro, F. R. 2007, *MNRAS*, 382, 443
- Martell, S. L., Smith, G. H., & Briley, M. M. 2008, *PASP*, 120, 7
- Mazzitelli, I., D’Antona, F., & Ventura, P. 1999, *A&A*, 348, 846
- Meynet, G., Ekström, S., & Maeder, A. 2006, *A&A*, 447, 623
- Milone, A. P., et al. 2008, *ApJ*, 673, 241
- Moehler S., Sweigart A.V., Landsman W.B., Hammer N.J., & Dreizler S. 2004, *A&A*, 415, 313
- Norris, J. E. 2004, *ApJ Letters*, 612, L25
- Origlia, L., & Leitherer, C. 2000, *AJ*, 119, 2018
- Pasquini, L., Bonifacio, P., Molaro, P., Francois, P., Spite, F., Gratton, R. G., Carretta, E., & Wolff, B. 2005, *A&A*, 441, 549
- Pasquini, L., Ecuivillon, A., Bonifacio, P., & Wolff, B. 2008, *ArXiv e-prints*, 806, arXiv:0806.3404
- Piersimoni, A. M., Bono, G., & Ripepi, V. 2002, *AJ*, 124, 1528
- Pilachowski, C. A., Sneden, C., Kraft, R. P., & Langer,

G. E. 1996, *AJ*, 112, 545

Piotto, G., Zoccali, M., King, I. R., Djorgovski, S. G., Sosin, C., Rich, R. M., & Meylan, G. 1999, *AJ*, 118, 1727

Piotto, G., et al. 2002, *A&A*, 391, 945

Piotto, G., et al. 2005, *ApJ*, 621, 777

Piotto, G., et al. 2007, *ApJ*, 661, L53

Pritzl, B. J., Smith, H. A., Catelan, M., & Sweigart, A. V. 2002, *AJ*, 124, 949

Pritzl, B. J., Smith, H. A., Stetson, P. B., Catelan, M., Sweigart, A. V., Layden, A. C., & Rich, R. M. 2003, *AJ*, 126, 1381

Raimondo, G., Castellani, V., Cassisi, S., Brocato, E., & Piotto, G. 2002, *ApJ*, 569, 975

Reimers, D. 1975, *Problems in stellar atmospheres and envelopes.*, 229

Rey, S.-C., Lee, Y.-W., Byun, Y.-I., & Chun, M.-S. 1998, *AJ*, 116, 1775

Richer, H. B., et al. 2006, *Science*, 313, 936

Rood, R. T., & Crocker, D. A. 1989, *IAU Colloq. 111: The Use of pulsating stars in fundamental problems of astronomy*, 103

Rosenberg, A., Recio-Blanco, A., & García-Marín, M. 2004, *ApJ*, 603, 135

Salaris, M., Weiss, A., Ferguson, J. W., & Fusilier, D. J. 2006, *ApJ*, 645, 1131

Salaris, M., & Weiss, A. 1998, *A&A*, 335, 943

Salaris, M., Cassisi, S., & Pietrinferni, A. 2008, *ApJ*, 678, L25

Sandquist, E. L., & Bolte, M. 2004, *ApJ*, 611, 323

Smith, G. H., Shetrone, M. D., Bell, R. A., Churchill, C. W., & Briley, M. M. 1996, *AJ*, 112, 1511

Suntzeff, N. 1993, *The Globular Cluster-Galaxy Connection*, 48, 167

Sweigart, A. V. 1997, in *Proc. Third Conference on Faint Blue Stars*, ed. A. G. D. Philip, J. Liebert, R. Saffer, & D. S. Hayes (Schenectady: L. Davis Press), 3

Sweigart, A. V., & Gross, P. G. 1976, *ApJ Suppl. Series*, 32, 367

van Albada, T. S., & Baker, N. 1973, *ApJ*, 185, 477

Ventura, P., Zeppieri, A., Mazzitelli, I., & D'Antona, F. 1998, *A&A*, 334, 953

Ventura, P., D'Antona, F., Mazzitelli, I., & Gratton, R. 2001, *ApJ Letters*, 550, L65

Ventura, P., D'Antona, F., & Mazzitelli, I. 2002, *A&A*, 393, 215

Ventura, P., & D'Antona, F. 2008, *MNRAS*, 255

von Braun, K., & Mateo, M. 2001, *AJ*, 121, 1522

Yong, D., & Grundahl, F. 2008, *ApJ*, 672, L29

Yoon, S.-J., Joo, S.-J., Ree, C. H., Han, S.-I., Kim, D.-G., & Lee, Y.-W. 2008, *ApJ*, 677, 1080

Walker, A. R. 1994, *AJ*, 108, 555

Walker, A. R. 1998, *AJ*, 116, 220

Wehlau, A., Slawson, R. W., & Nemec, J. M. 1999, *AJ*, 117, 286

Weiss, A., Denissenkov, P. A., & Charbonnel, C. 2000, *A&A*, 356, 181

Welty, D. E. 1985, *AJ*, 90, 2555

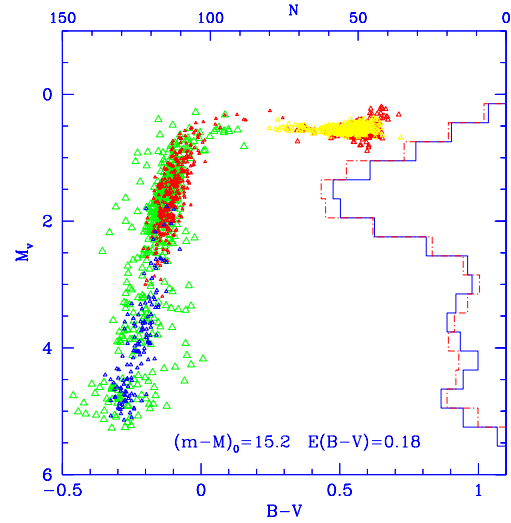


Figure A1. The HB data by Bedin et al. (2000) (open triangles) and their simulation superimposed (full triangles). The histogram of the blue HB data is shown as a full histogram on the right, and the simulated histogram is dot-dashed. The lower luminosity clumps EBT2 and EBT3 are both obtained with a unique value of $Y=0.385$, as explained in the text.

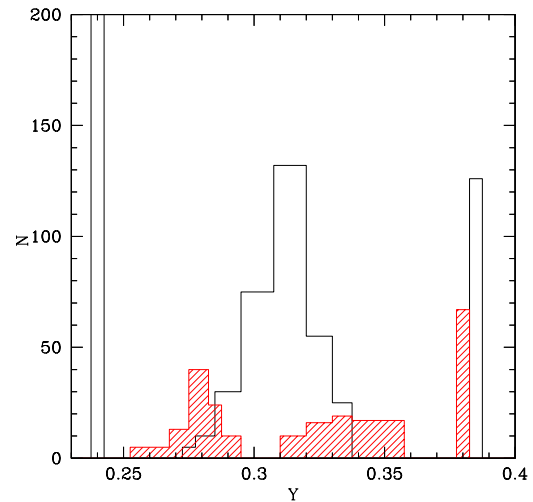


Figure A2. The full histogram represents the number vs. helium content distribution of the NGC 2808 HB of Fig. A1. The dashed histogram represents the corresponding distribution for M 13. Notice that the M 13 distribution completely lacks stars with normal $Y=0.24$.

APPENDIX A: A NEW ANALYSIS OF NGC 2808 OPTICAL AND ULTRAVIOLET DATA

A1 The V vs. B-V data

We analyzed the Bedin et al. (2000) data of NGC 2808 twice (D'Antona & Caloi 2004; D'Antona et al. 2005), but always assuming that the mass lost on the RGB has a slight but positive dependence on the helium content of the sample. Having now shown that this is not the case (Sect. 2) it is reasonable to make another analysis, and derive the

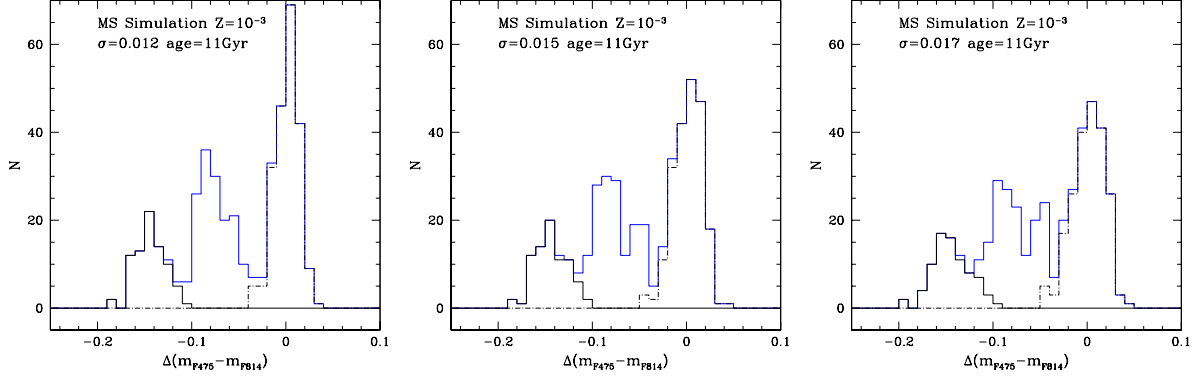


Figure A3. The figures show simulation of the main sequence colour distribution corresponding to the $N(Y)$ distribution of Fig. A2 in the ACS colour F475-F814 of Piotto et al. 2007. The simulation is shown for the magnitude interval $5.0 \leq M_{814} \leq 6.0$. The three panels correspond to different assumed errors on the colour (0.012, 0.015 and 0.017mag).

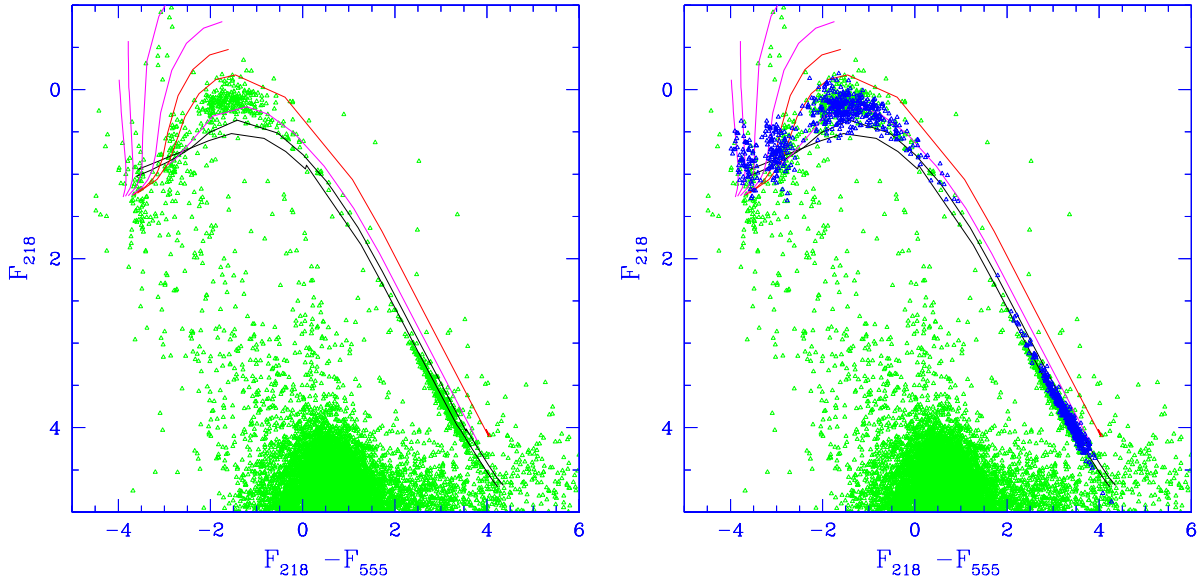


Figure A4. We show the ZAHBs of $Z=0.001$ with different helium content in the absolute UV magnitude F_{218} versus $F_{218}-F_{555}$ colour. The $Y=0.24$ ZAHB line is used to define the distance modulus and reddening of the dataset by Castellani et al. 2005. We impose that the red clump data (on the right bottom part of the left figure) lie symmetrically on this ZAHB. The rising lines on the left are ZAHBs of models with the same core mass of the $Y=0.40$ sequence, but having larger envelope helium abundance. From left to right, we have $Y=0.8, 0.7, 0.6, 0.5$ and 0.45 . On the right, we show the simulation of Fig. A1.

$N(Y)$ distribution that fits the HB, obtained by assuming that both δM_0 and σ do not depend on Y . For the simulation, we closely follow the procedure by D’Antona & Caloi (2004) and D’Antona et al. (2005), apart from the analysis of the blue hook stars (the clump EBT3 in the definition by Bedin et al. 2004) for which we make the further assumptions described below. The problem is that we *can not adopt a different helium content for each of the clumps EBT2 and EBT3*, because, using the $N(Y)$ distribution that reproduces the HB, we have to reproduce also the colour distribution in the MS data by Piotto et al. (2007). For this aim, we convert our main sequence stellar models into the ACS bands F475 and F814 by means of the transformations provided by Bedin et al. (2005), and simulate the MS colour distribution. We can not make a detailed comparison with the

data, as they are not available to us, but simply show the histogram of number versus the colour difference (in F475–F814) from the reference main sequence of $Y=0.24$, in the magnitude interval $5 \leq M_{814} \leq 6$. Comparison with the histograms in Figure 3 in Piotto et al. (2007) shows that there is a fair reproduction of the observations, if the colour error is taken to be 0.017mag (indicated by σ in the top of Fig. A3).

Let us discuss in detail the assumptions made to fit the EBT2 and EBT3 clumps. As the blue MS is well separated from the other stars, all the stars in this blue MS share the same helium abundance. We then take a unique high helium abundance for all the stars in the clumps EBT2 and EBT3 (as we assumed also in D’Antona et al. 2005). Attributing to the cluster an age of 11Gyr, the average mass loss rate

necessary to fit the red clump is $0.18 M_{\odot}$. Due to the spread in mass loss ($\sigma=0.008 M_{\odot}$) assumed in order to fit the width of the red clump, and due to the choice of a very high helium in order to reproduce the blue MS, the remnant mass is in a very strict range close to the helium flash mass ($M \sim 0.49 M_{\odot}$, to be compared with $M_c=0.4676 M_{\odot}$, for $Y=0.40$). We will fix a value M_{mixing} , above which we put the star on the track corresponding to its mass and helium content. Below M_{mixing} , we assume that the star has suffered very deep mixing, and that *its helium surface abundance has increased*. We parametrize the resulting surface helium abundance between fixed values, and distribute random the stars along the corresponding tracks. By this hypothesis, we are able to reproduce well the gap between EBT2 and EBT3 *without invoking a helium discontinuity*, as shown in Fig. A1. We summarize the parameters chosen for this fit: age of 11 Gyr, $\Delta M_0 = 0.18 M_{\odot}$, $\sigma = 0.008$, $M_{mixing}=0.487 M_{\odot}$, and the $N(Y)$ is shown in Fig. A2.

A2 The HST UV data of NGC 2808

The optical bands are certainly not the best to describe the very hot HB stars in NGC 2808. The HST data have shown that these objects are the most luminous ones in the UV bands (Brown et al. 2001). Lee et al. (2005) first attempted to fit the data with HB models having varying helium content. Here we use the data by Castellani et al. (2006) in the plane F218 versus the colour F218-F555. Our models have been transformed into these bands by using the Origlia & Leitherer (2000) colour transformations. Fig. B1 shows on the left the data and the ZAHBs. The choice of the distance modulus and reddening in the colour F218-F555 have been made in order to fit the red clump data on the $Y=0.24$ ZAHB. This choice leads to a good superposition of the highest luminosity stars (corresponding to the EBT1 clump by Bedin et al. 2004) above the ZAHB of $Y=0.32$. The rising short lines on the left are ZAHBs of models with the same core mass of the $Y=0.40$ sequence, but having larger envelope helium abundance. From left to right, we have $Y=0.8, 0.7, 0.6, 0.5$ and 0.45 . The simulation shown in Fig A1 for the B and V colours is shown in the right part of Fig. A4 in these UV bands. The fit of red clump, EBT1 and EBT2 is very good, showing once for all that there is a helium difference between the red clump, EBT1 and EBT2. The gap between EBT2 and EBT3 results well simulated by assuming that a fraction of the stars born with $Y=0.40$ suffers deep mixing, increasing its Y to the range $Y=0.7-0.8$. Nevertheless, the simulation fails to reproduce the lowest luminosity EBT3 stars. Reasons for this result are several: first of all, these stars have atmospheres which are not only very helium rich as we assumed, but also carbon rich, and the T_{eff} -colour transformations can not take this into account. Second, it is well possible that these stars ignite helium with a late flash at a core mass smaller than we assumed, and thus have a smaller intrinsic luminosity.

APPENDIX B: A POSSIBLE FIT FOR THE HB OF M 13

Caloi & D'Antona (2005) provocatively proposed that the blue-HB clusters, and in particular M 13, have completely

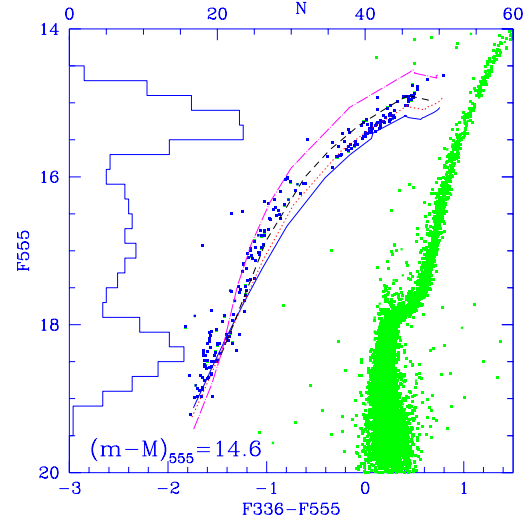


Figure B1. M 13 HB data by Ferraro et al.(1998) compared with our ZAHBs in the plane F555 vs. F336-F555. The distance modulus is chosen so that the $Y=0.28$ ZAHB (dotted line) fits the upper luminosity clump. The other lines are the ZAHBs for $Y=0.24$ (full line), $Y=0.32$ (dashed) and $Y=0.40$ (dash dotted). On the left we show the histogram of HB counts as a function of F555 magnitude.

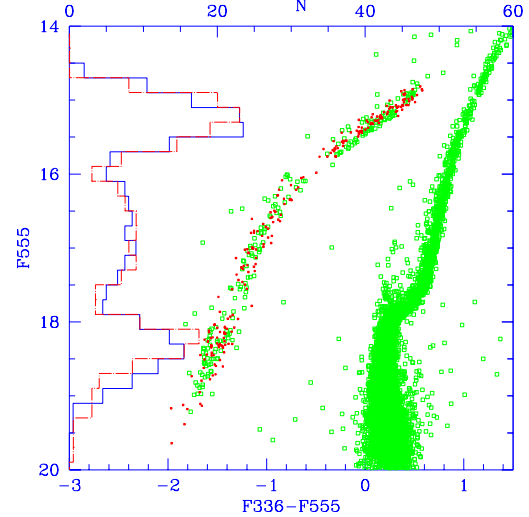


Figure B2. Superimposed to the data, we show the simulation done with the same values, $\delta M=0.18 M_{\odot}$ and age 11 Gyr, chosen for the NGC 2808 simulation. σ is $0.01 M_{\odot}$ and $M_{mixing}=.479 M_{\odot}$

lost their FG (see Sect. 6.1). As the metallicity of M 13 and NGC 2808 are close, and the blue HB of the two clusters are morphologically similar, we try to fit the HB of this cluster by imposing a simulation in which the age and average mass loss are the same as in the NGC 2808 fit, but *the red clump population, at $Y=0.24$, is totally eliminated*. Fig.B1 shows the HST data by Ferraro et al. (1998) in the plane F555 vs. F336-F555. We superimpose our ZAHBs as in Fig. B1, assuming a visual distance modulus of 14.6mag and zero reddening. The modulus is chosen so that the $Y=0.28$ ZAHB coincides with the upper clump, in agree-

ment with the result by Caloi & D'Antona (2005) that attributed $Y=0.28$ to the dominant cluster population. We see that, with this choice, the ZAHB of the middle HB is again consistent with $Y\sim 0.32$. This difficulty of fitting the HB with a unique ZAHB had already been pointed out by Grundahl et al. (1998) in their analysis of the HR diagram of M 13 in the Strömgren colours, and signalled also for the clusters NGC 288 and NGC 6752. These authors indeed attributed this unexpected feature to the presence in M 13 of two distinct HB populations, one of which had undergone deep mixing, following Sweigart (1997). In our interpretation, these stars have a higher helium content already starting from their formation.

Fig. B2 shows the HB simulation superimposed to the M 13 data. Apart from the lack of the $Y=0.24$ part, the distribution $N(Y)$ is different indeed from that obtained for NGC 2808, as we show in Fig. A2, but the lowest part of the HB can be interpreted again as a very high helium population ($Y=0.38$). Notice however, that M 13 does not contain the large population of blue hook stars present in NGC 2808, and this difference remains to be explained.